Dyes and Pigments 91 (2011) 105–111

Contents lists available at ScienceDirect

Dyes and Pigments

journal homepage: www.elsevier.com/locate/dyepig

Azo-hydrazone tautomerism by *in situ* Cu^{II} ion catalysis and complexation with the H_2O_2 oxidant of C.I. Disperse Yellow 79

Bin Hu, Gang Wang, Wei You, Wei Huang*, Xiao-Zeng You

State Key Laboratory of Coordination Chemistry, Nanjing National Laboratory of Microstructures, School of Chemistry and Chemical Engineering, Nanjing University, Nanjing 210093, PR China

ARTICLE INFO

Article history:
Received 19 January 2011
Received in revised form
14 March 2011
Accepted 14 March 2011
Available online 21 March 2011

Keywords:
Azo-hydrazone tautomerism
Disperse azo dyes
C.I. Disperse Yellow 79
Cu^{II} ion catalysis
$\pi-\pi$ Stacking interactions
Dye-metal complexes

ABSTRACT

A novel dinuclear copper(II) complex **2** bearing double μ_2-oxo bridges has been obtained by *in situ* Cu^{II} ion catalysis and complexation with the H_2O_2 oxidant of C.I. Disperse Yellow 79 (**1**), where a new dianionic ligand is *in situ* formed having an additional phenolic group and it coordinates with the central Cu^{II} ion as a tridentate chelating ligand. Furthermore, both of the starting material **1** and the final neutral dye-metal product **2** have been structurally and spectrally characterized and compared, where azo-hydrazone tautomerism has been observed before and after metal-ion complexation. To the best of our knowledge, this is the first structural report about the heterocyclic dyes having quinoline-2,4-dione skeleton and the corresponding azo-hydrazone tautomerism between them.

1. Introduction

Significant progress has been made over the past years in the area of azo dyes and their metal complexes because of their wide versatility in textile dyeing and polyamide fiber coloring [1–4]. Recently, azo compounds are known to be involved in a number of biological reactions [5], nonlinear optical elements [6,7], printing systems [8] and optical storage of information [9,10]. Aromatic heterocycles azo dyes have shown brilliant color and chromophoric strength, especially for their excellent properties on light and sublimation fastness [11,12]. C.I. Disperse Yellow 79 (**1**) having 1-methyl-quinoline-2,4-dione backbone is one of them showing excellent textile discharge printing property for polyester fiber. As for some azo dyes having aromatic coupling components, it has been proved that one hydroxyl group can be added to the aromatic unit forming an oxidized azo compound and its dye-metal complexes in the presence of H_2O_2 and a Cu^{II} ion, which is directed by the electronic effects of their substituted group(s) [13]. The introduction of an electron-withdrawing phenolic group and a metal center into the dye molecule can improve the electron acceptor behavior of azo chromophore and the delocalized π-system of resulting dye molecules [14,15].

X-ray single-crystal diffraction is a very powerful tool to investigate tautomerisms because it provides detailed information on molecular conformation and supramolecular interactions in the solid state [16–18]. We have previously reported structural, spectral and density function theory computational studies of a series of C.I. Disperse Yellow dyes (114, 119, 126, 211, 241) having the same 1-alkyl-5-cyano-2-hydroxy-4-methyl-6-pyridone coupling components, and our results demonstrate that this family of dyes exists in the hydrazone form instead of the conventionally regarded azo form both at 120 and 291 K [19–22]. In addition, we have mentioned the first observation of azo-hydrazone and cis-trans tautomerisms for Disperse Yellow dyes and their nickel(II) and copper(II) complexes, where two cyano-extended one-dimensional copper(II) dye-metal coordination polymers are described [22]. Now we are further exploring the conformational investigations on aromatic heterocyclic disperse dyes as well as preparation and properties of new dye-metal complexes.

As an extensive study in this area, we select herein a cyano-free heterocyclic dye (**1**) bearing a different 1-methyl-quinoline-2,4-dione backbone and characterize its structure. Furthermore, we prepare a novel dinuclear copper(II) complex (**2**) by *in situ* Cu^{II} ion catalysis and complexation with the H_2O_2 oxidant of **1**, and study the azo-hydrazone tautomerism and alteration of spectral properties between

* Corresponding author. Tel.: +86 25 83686526; fax: +86 25 83314502.
E-mail address: whuang@nju.edu.cn (W. Huang).

0143-7208/$ – see front matter © 2011 Elsevier Ltd. All rights reserved.
doi:10.1016/j.dyepig.2011.03.017

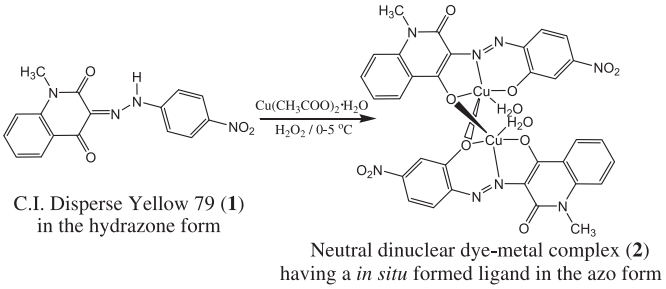

Scheme 1. Schematic illustration of the preparation of dinuclear Cu^{II} complex **2** where chemical azo-hydrazone tautomerism between the pyridine-2,6-dione form in **1** and the 2-hydroxy-6-pyridone form in the *in situ* formed ligand in **2** takes place before and after metal-ion complexation.

1 and **2** before and after metal-ion complexation (Scheme 1). By checking the latest version of CCDC databases (CSD version of 5.32 updated to November 2010) on quinoline-based azo dyes, it is found that there is only one structural report on a copper(II)-hydrazone complex of *N*-(4-methyl-quinolin-2-yl)-*N*′-(phenyl-pyridin-2-yl-methylene)-hydrazine, which is suggested to be potentially anti-cancer and anti-inflammatory [23]. So this work is the first structural report on the aromatic heterocyclic dyes having quinoline-2,4-dione skeleton and corresponding azo-hydrazone tautomerism between the dye molecule and its neutral dye-metal complex.

2. Experimental section

2.1. Materials and measurements

C.I. Disperse Yellow 79 (**1**) was purchased directly from commercial sources. All other reagents and solvents were of analytical grade and used without further purification. Acceptable yellow single crystals of **1** suitable for X-ray diffraction measurement were produced by slow evaporation of its methanol solution after several weeks in air at room temperature.

Elemental analyses (EA) for carbon, hydrogen, and nitrogen were performed on a Perkin–Elmer 1400C analyzer. ^{1}H NMR spectra were obtained in a Bruker 500 MHz NMR spectrometer. Infrared (IR) spectra (4000–400 cm^{-1}) were recorded using a Nicolet FT-IR 170X spectrophotometer on KBr disks. Electrospray ionization mass spectra (ESI-MS) were recorded on a Finnigan MAT SSQ 710 mass spectrometer in a scan range of 200–2000 amu. UV–Vis spectra were recorded with a Shimadzu UV-3150 double-beam spectrophotometer using a Pyrex cell with a path length of 10 mm. Powder X-ray diffraction (PXRD) measurements were performed on a Philips X'pert MPD Pro X-ray diffractometer using Cu $K\alpha$ radiation ($\lambda = 0.15418$ nm), in which the X-ray tube was operated at 40 kV and 40 mA at room temperature. TGA–DSC (thermogravimetry analysis–differential scanning calorimeter) experiments were carried out by a NETZSCH STA449C thermogravimetric analyzer instrument in the nitrogen flow from 10 to 800 °C at a heating rate of 10.0 °C min^{-1}.

2.2. Preparation of dinuclear copper(II) complex **2**

$Cu(CH_3COO)_2 \cdot H_2O$ (0.042 g, 0.21 mmol) and C.I. Disperse Yellow 79 (0.068 g, 0.21 mmol) were dissolved in 30 cm^3 *N*,*N*′-dimethylformamide and the mixture was cooled to 0 °C with ice water bath, and then an aqueous solution of 30% hydrogen peroxide (6 cm^3) was added dropwise in order that the temperature of

Table 1
Crystal and structural refinement data for compounds **1** and **2**.

Compound	**1**	**2**
Empirical formula	$C_{16}H_{12}N_4O_4$	$Cu_2C_{32}H_{24}N_8O_{12}$
Formula weight	324.30	839.69
Crystral size (mm)	0.12 × 0.10 × 0.10	0.10 × 0.10 × 0.10
Crystal system	Triclinic	Triclinic
Space group	$P\bar{1}$	$P\bar{1}$
a, Å	7.8700(14)	7.7302(12)
b, Å	8.0484(15)	8.2404(12)
c, Å	11.469(2)	13.782(2)
α, deg	94.770(2)	89.723(2)
β, deg	92.856(3)	83.928(1)
γ, deg	95.972(2)	62.528(2)
V, Å^3	718.8(2)	773.6(2)
Z/D_{calcd} (Mg m^{-3})	2/1.498	1/1.802
F(000)	336	426
μ (mm^{-1})	0.870	1.459
max/min transmission	0.9895/0.9838	0.8678/0.8218
h_{min}/h_{max}	−8/9	−9/9
k_{min}/k_{max}	−9/9	−8/9
l_{min}/l_{max}	−9/13	−13/16
Absorption correction	Multi-scan	Multi-scan
Data collected /unique	3625/2499	3870 /2679
Final *R* indices [$I > 2\sigma(I)$]	$R1 = 0.0440$, $wR2 = 0.1222$	$R1 = 0.0476$, $wR2 = 0.1071$
R indices (all data)	$R1 = 0.1019$, $wR2 = 0.1375$	$R1 = 0.0801$, $wR2 = 0.1481$
S	0.941	0.950
Δ/e Å^{-3} (max, min)	0.169/−0.137	0.495/−0.535

$R_1 = \Sigma||Fo| - |Fc||/\Sigma|Fo|$, $wR_2 = [\Sigma[w(Fo^2 - Fc^2)^2]/\Sigma w(Fo^2)^2]^{1/2}$.

Table 2
Bond lengths [Å] and angles [°] for compounds **1** and **2**.

1		**2**	
C1–N2	1.320(3)	Cu1–O2	1.893(4)
C1–C2	1.467(3)	Cu1–N3	1.928(4)
C1–C5	1.471(3)	Cu1–O5	1.938(3)
C2–O1	1.242(2)	Cu1–O6	2.034(3)
C2–N1	1.369(3)	Cu1–O5^a	2.267(4)
C3–N1	1.407(3)	Cu1–Cu1^a	3.129(1)
C5–O2	1.231(3)	C1–N2	1.380(7)
C10–N1	1.461(3)	C1–C5	1.413(7)
C11–N3	1.402(3)	C1–C2	1.468(7)
C14–N4	1.457(3)	C2–O1	1.252(6)
N2–N3	1.298(2)	C2–N1	1.346(7)
N4–O4	1.222(3)	C3–N1	1.405(6)
N4–O3	1.226(3)	C5–O2	1.287(6)
		C10–N1	1.473(7)
N2–C1–C2	124.3(2)	C11–N3	1.399(7)
N2–C1–C5	114.8(2)	C12–O5	1.335(6)
C2–C1–C5	120.9(2)	C14–N4	1.479(7)
O1–C2–N1	120.8(2)	N3–N2	1.290(6)
O1–C2–C1	120.7(2)	N4–O4	1.219(6)
N1–C2–C1	118.5(2)	N4–O3	1.224(6)
C6–C3–N1	119.6(2)	O5–Cu1^a	2.267(4)
C4–C3–N1	120.8(2)		
O2–C5–C4	121.9(2)	O2–Cu1–N3	91.8(2)
O2–C5–C1	122.0(2)	O2–Cu1–O5	176.3(2)
C4–C5–C1	116.1(2)	N3–Cu1–O5	84.8(2)
C16–C11–N3	118.1(2)	O2–Cu1–O6	93.5(2)
C12–C11–N3	121.4(2)	N3–Cu1–O6	148.9(2)
C13–C14–N4	119.7(3)	O5–Cu1–O6	90.2(2)
C15–C14–N4	119.2(3)	O2–Cu1–O5^a	96.7(2)
C2–N1–C3	122.4(2)	N3–Cu1–O5^a	122.6(2)
C2–N1–C10	118.4(2)	O5–Cu1–O5^a	84.2(2)
C3–N1–C10	119.2(2)	O6–Cu1–O5^a	87.1(1)
N3–N2–C1	119.8(2)	O2–Cu1–Cu1^a	134.6(1)
N2–N3–C11	120.3(2)	N3–Cu1–Cu1^a	109.5(1)
O4–N4–O3	122.7(2)	O5–Cu1–Cu1^a	46.1(1)
O4–N4–C14	118.4(3)	O6–Cu1–Cu1^a	88.0(1)
O3–N4–C14	118.9(3)	O5a–Cu1–Cu1^a	38.0(1)
		Cu1–O5–Cu1^a	95.8(2)

Symmetry code: $a = -x + 1, -y, -z + 1$.

Table 3
Hydrogen bonding parameters (Å, °) in compounds **1** and **2**.

D–H···A	D–H	H···A	D···A	∠DHA	Symmetry code
1					
N3–H3···O1	0.86	1.89	2.570(2)	135	
C7–H7···O4	0.93	2.52	3.430(4)	166	$x-1, 1+y, z-1$
C10–H10C···O2	0.96	2.59	3.433(3)	146	$x, 1+y, z$
2					
O6–H6A···O1	0.85	1.94	2.736(6)	155	$-x, -y, 1-z$
O6–H6B···O1	0.85	2.09	2.879(6)	155	$1+x, y-1, z$
C8–H8···O4	0.93	2.53	3.222(8)	131	$x, y-1, 1+z$
C16–H16···O6	0.93	2.58	3.506(7)	171	$x-1, 1+y, z$

reaction mixture did not exceed 5 °C. The color of solution turned out to be vermillion after 10 mins' reaction, and the mixture was stirred at 0–5 °C for 5 h. The mixture was then filtered and the filtrate was condensed to 5 cm^3 by a rotatory evaporator. The

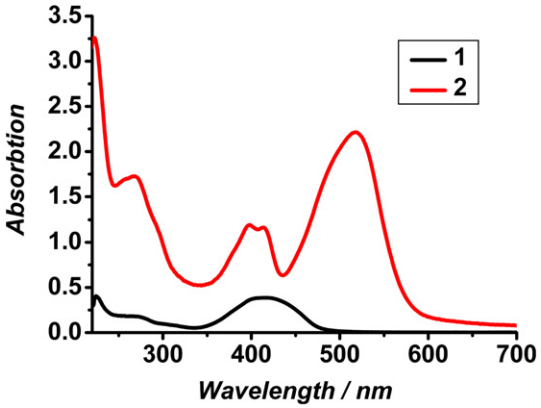

Fig. 2. UV–Vis spectra of the **1** and **2** in their 5.0×10^{-5} mol/L methanol solutions.

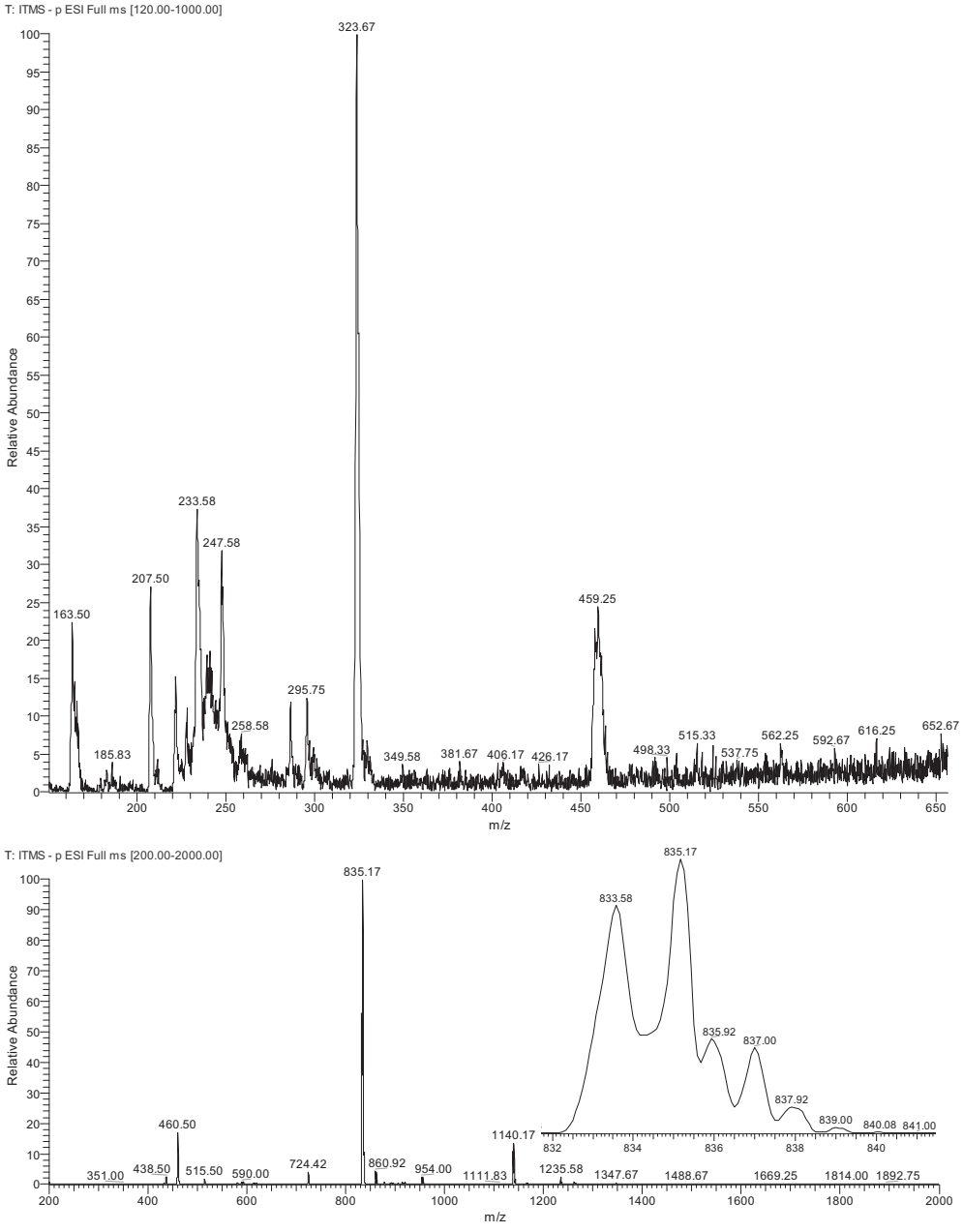

Fig. 1. ESI-MS spectra of compounds **1** (a) and **2** (b) in the negative ion mode.

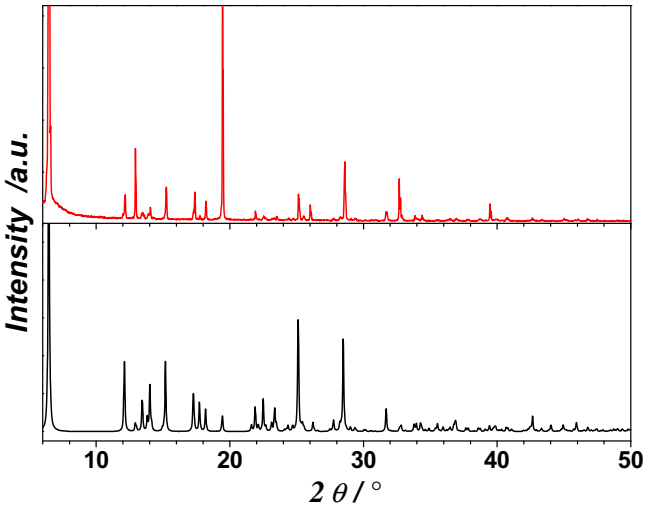

Fig. 3. The simulative (black line) and experimental (red line) powder X-ray diffraction patterns for dinuclear copper(II) complex **2** (For interpretation of the references to color in this figure legend, the reader is referred to the web version of this article.).

residue was filtered and the black precipitates were filtered, washed by methanol and dried in vacuo. Yield: 0.051 g (56.5%) based on metal. Red brown single crystals of 2 suitable for X-ray structural analysis were obtained from a mixture of DMF and methanol in a ratio of 1:3 (v/v) via 15 days' slow evaporation in air at room temperature. Elemental anal. Calcd for $Cu_2C_{32}H_{24}N_8O_{12}$: C, 45.77; H, 2.88; N, 13.35%. Found: C, 45.96; H, 3.09; N, 13.11%. Main FT-IR absorptions (KBr pellets, ν, cm^{-1}): 3400(b), 1601(vs), 1503(vs), 1441(m), 1411(m), 1365(m), 1331(vs), 1308(vs), 1249(w), 1216(m), 1126(s), 1067(m), 874(m), 817(m), 759(m) and 616(m). UV/Vis in methanol: $\lambda_{max} = 222$ (65205), 268 (34542), 398 (23846), 414 (23278) and 518 (44256) nm. Negative ion ESI-MS in methanol (m/z): 835.17 (100%).

2.3. X-ray data collection and solution

Single-crystal samples of **1** and **2** were glue-covered and mounted on glass fibers for data collection on a Bruker SMART 1K CCD area detector at 291(2) K using graphite mono-chromated Mo

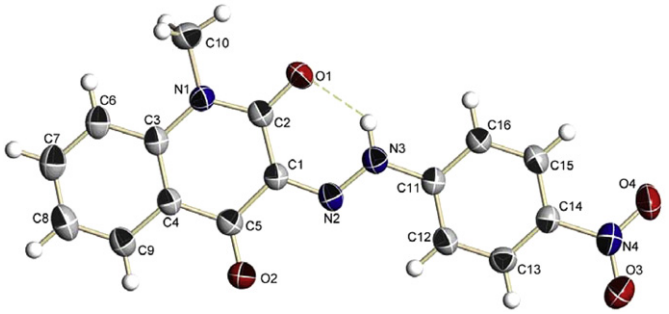

Fig. 5. ORTEP drawing of C.I. Disperse Yellow 79 (**1**) with the atom-numbering scheme. Displacement ellipsoids are drawn at the 30% probability level.

Kα radiation ($\lambda = 0.71073$ Å). The collected data were reduced by using the program SAINT [24] and empirical absorption corrections were done by SADABS [25] program. The crystal systems were determined by Laue symmetry and the space groups were assigned on the basis of systematic absences by using XPREP. The structures were solved by direct method and refined by least-squares method. All non-hydrogen atoms were refined on F^2 by full-matrix least-squares procedure using anisotropic displacement parameters, while hydrogen atoms were inserted in the calculated positions assigned fixed isotropic thermal parameters at 1.2 times of the equivalent isotropic U of the atoms to which they are attached (1.5 times for the methyl groups) and allowed to ride on their respective parent atoms. All calculations were carried out on a PC computer with the SHELXTL PC program package [26] and molecular graphics were drawn by using XSHELL, XP and ChemDraw software. The summary of the crystal data, experimental details and refinement results for **1** and **2** is listed in Table 1. Selected bond distances and bond angles are given in Table 2, while versatile hydrogen bonding interactions in **1** and **2** are listed in Table 3.

3. Results and discussion

3.1. Syntheses and spectral characterizations

In this work, a novel dinuclear copper(II) complex (**2**) has been successfully yielded by the excess H_2O_2 oxidation of C.I. Disperse

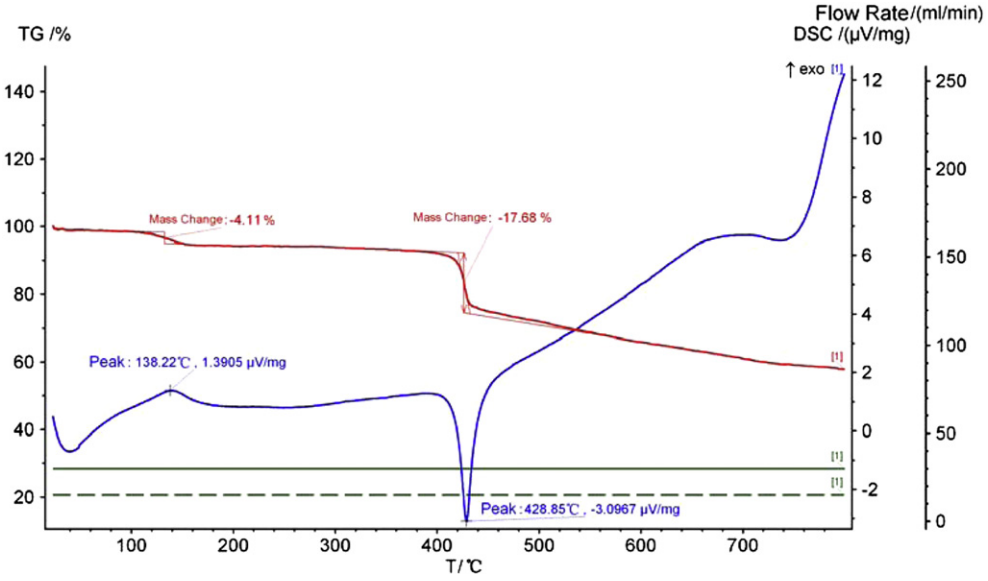

Fig. 4. Diagram of TGA-DSC for complex **2**.

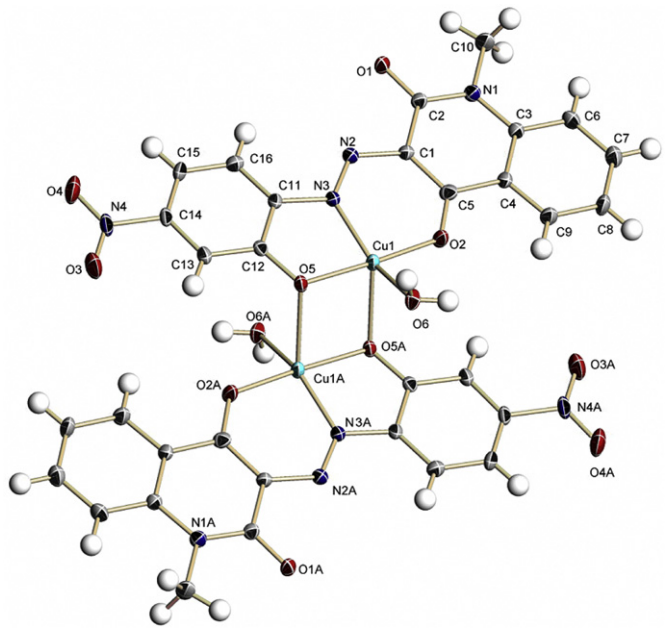

Fig. 6. ORTEP drawing of **2** with the atom-numbering scheme. Displacement ellipsoids are drawn at the 30% probability level.

Yellow 79 (**1**) in the presence of a Cu^{II} ion, where the Cu^{II} ion acts as a catalyst and a metal center for complexation simultaneously. Compared with **1**, a new ligand in **2** is *in situ* formed bearing an additional phenolic group, where a new coordination site of phenolic O atom is generated. Negative ion ESI-MS studies of **1** and **2** give molecular ion peaks at $m/z = 323.75$ (100% strength for **1**) and 835.17 (100% strength for **2**), respectively, as can be seen in Fig. 1. Moreover, ^{1}H NMR spectrum of **1** in the $CDCl_3$ solvent exhibits a single peak at 16.27 ppm, indicative of the existence of a hydrazone proton.

UV–vis spectra of azo dyes are generally affected by their chemical structures such as chromophores, substituted groups, number of azo groups, metal ions, pH values, solvents and so on [27–30]. In order to explore and compare the differences of **1** and **2** before and after Cu^{II} ion *in situ* catalysis and complexation, UV–vis spectra of **1** and **2** in their 5.0×10^{-5} mol/L methanol solutions are determined, and the results are shown in Fig. 2. Yellow compound **1** shows a broad absorption peak centered at 415 nm, which can be assigned as typical $\pi-\pi^*$ transitions between the aromatic rings and the azo unit of dye molecule. In contrast, the $\pi-\pi^*$ transition absorption peak of red brown complex **2** is red-shifted to 518 nm exhibiting a large bathochromic shift of 103 nm. Furthermore, the molar extinction coefficients of **2** at 222 and 518 nm ($\varepsilon = 65{,}205$ and 44,256) are significantly increased compared with those of **1** at 224 and 416 nm ($\varepsilon = 8076$ and 7724). In addition, a splitting of the $n-\pi^*$ transition of the conjugated chromophore is observed at 398 and 414 nm in **2**. The strong hyperchromic effects after metal-ion complexation cannot be ascribed to *d–d* electron transitions of the Cu^{2+} ions, which are generally too weak and may easily be obscured by the strong absorption band of the azo ligand [31–33]. In this case, they are believed to originate from at least two aspects: On the one hand, the presence of an additional electron-attracting phenolic group in the *in situ* formed dianionic ligand showing planar tridentate chelating coordination fashion; On the other hand, the construction of stable fused five-membered and six-membered chelating rings in dinuclear copper(II) complex **2** and the delocalization of lone electron pairs of N and O coordination atoms after the formation of multiple coordination bonds.

The pure phase of dinuclear copper(II) complex **2** is also confirmed by PXRD patterns as illustrated in Fig. 3. TGA–DSC study of **1** reveals that it starts to decompose from 200 °C with an exothermic DSC peak at 262 °C. In comparison, DTA–DSC study of 2 shows a 4.11% weight loss (Calcd. 4.29%) in the range of 95–165 °C with an exothermic DSC peak at 138 °C (Fig. 4), corresponding to the loss of two coordination water molecules. After that it can keep unchangeable till 420 °C, and finally it starts to decompose with a sharp endothermic DSC peak at 429 °C. Here one can see that the thermal stability of dinuclear copper(II) complex **2** is much higher than that of C.I. Disperse Yellow 79 after metal-ion complexation.

3.2. Structural description of Disperse Yellow azo dye *1*

The molecular structure of **1** with atom-numbering scheme is shown in Fig. 5. It crystallizes in the triclinic $P\bar{1}$ space group without the presence of any solvent molecule. As a common feature of azo dyes, all the non-hydrogen atoms in **1** are essentially coplanar with the mean deviation from least-squares plane of 0.026(3) Å. The dihedral angle between the phenyl and the quinoline rings is 1.2(2)°. The whole dye molecule adopts the *Z* configuration and the methyl group bonded to the quinoline nitrogen atom is positioned at the same side of the H3 atom of N3. Like our previously reported 1-alkyl-5-cyano-2-hydroxy-4-methyl-6-pyridone based C.I. Disperse Yellow dyes, 1-methyl-quinoline-2,4-dione based C.I. Disperse Yellow dye 79 also exhibits the hydrazone form in the solid state, which can be deduced from the related bond lengths. Additionally, an obvious Q peak is found near atom N3 when solving the structure, where the X-ray diffraction data are in the high quality. Furthermore, the hydrazone hydrogen atom is involved in the intramolecular hydrogen bonding with the oxygen atom (O2) at 2-position of quinoline group forming a six-membered hydrogen-bonded ring.

Strong $\pi-\pi$ stacking and weak intermolecular C–H···O hydrogen bonding interactions can be observed in the crystal packing of **1**. As shown in Fig. 6, three kinds of offset $\pi-\pi$ stacking interactions are found between the phenyl and the quinoline rings from contiguous molecules with the centroid-to-centroid contacts of 3.502(3), 3.843(3) and 4.066(3) Å, respectively, forming an ordered layer packing structure.

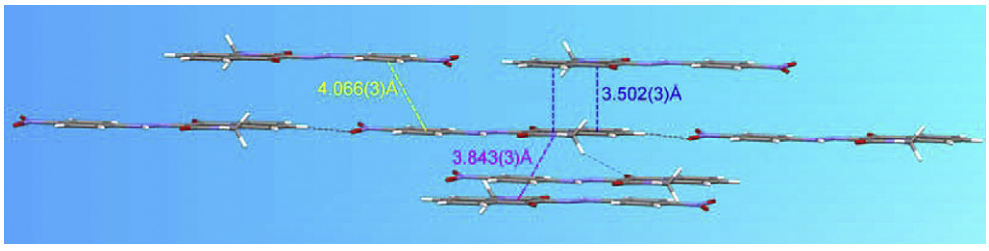

Fig. 7. Perspective view of $\pi-\pi$ stacking and hydrogen bonding interactions in the layer packing structure of **1**.

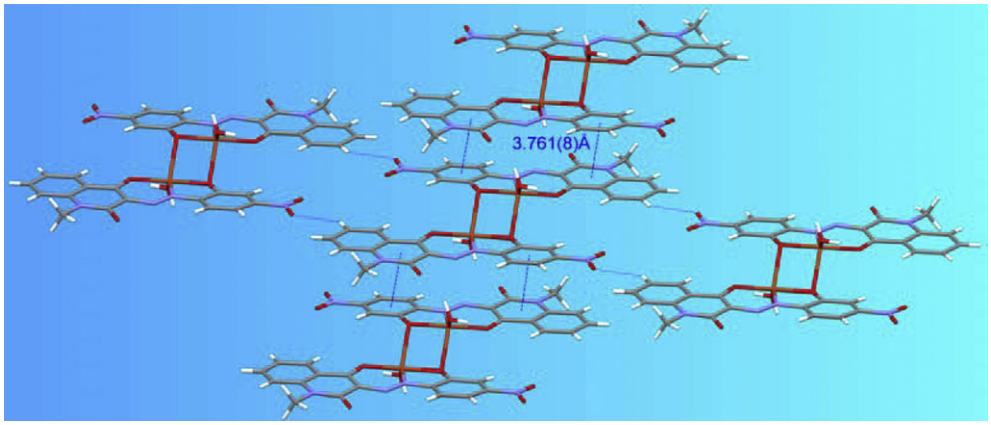

Fig. 8. Perspective view of $\pi-\pi$ stacking and hydrogen bonding interactions in the packing structure of **2**.

3.3. Structural description of neutral dye-metal complex **2**

The molecular structure of neutral dye-metal complex **2** with atom-numbering scheme is shown in Fig. 7. It also crystallizes in the triclinic $P\bar{1}$ space group. The dianion of oxidant of **1** in this case serves as a tridentate chelating ligand, and one of the oxygen atoms (O5) adopts a μ_2-bridging mode linking adjacent two Cu^{II} centers. Thus, a dinuclear copper(II) complex bearing double μ_2-oxo bridges is formed where another coordination water molecule occupies the fifth coordination site. The separation between Cu1···Cu1A ($1-x$, $-y$, $1-z$) is 3.129(1) Å, and the coordination geometry of each copper(II) ion is severely Jahn-Teller distorted pyramidal with a τ value of 0.456 [34]. The apical Cu1–O5A bond length is 2.267(4) Å, which is much longer than the other four Cu–O and Cu–N bond lengths in the basal plane (1.893(4)–2.034(3) Å).

In this *in situ* formed dianionic tridentate chelating ligand, all the non-hydrogen atoms are also essentially coplanar with the mean deviation from least-squares plane of 0.049(6) Å. The dihedral angle between the phenyl and the quinoline rings is 5.0(2)° and the oxygen atom of coordination water molecule (O6) is 1.076(6) Å above the least-squares plane.

It is worthwhile to mention that chemical azo-hydrazone tautomerism between the pyridine-2,6-dione form in **1** and the 2-hydroxy-6-pyridone form in the *in situ* formed ligand in **2** takes place before and after metal-ion complexation, which is evidenced by the variation of related bond lengths. The continuously connected N3–N2, N2–C1, C1–C2 and C2–O1 bond lengths in **1** are 1.298(2), 1.320(3), 1.467(3) and 1.242(2) Å. In contrast, these four bond lengths in **2** are elongated or shortened as 1.290(6), 1.380(7), 1.468(7) and 1.252(6) Å, indicative of the shifts of partially delocalized single and double-bond character.

As can be seen in Fig. 8, $\pi-\pi$ stacking interactions are observed between the phenyl and the quinoline rings of neighboring dinuclear copper(II) molecules. They are packed in a head-to-tail fashion with the centroid-to-centroid separations of 3.761(8) Å. In addition, the structure is further stabilized by strong O–H···O intermolecular hydrogen bonds between both of the hydrogen atoms of water molecule and one of the oxygen atoms (O1) of quinoline unit.

4. Conclusion

In summary, a novel dinuclear copper(II) complex **2** bearing double μ_2-oxo bridges has been obtained by *in situ* Cu^{II} ion catalysis and complexation with the H_2O_2 oxidant of **1**, where a new ligand is *in situ* formed having an additional phenolic group and it coordinates with the central Cu^{II} ion as a tridentate chelating ligand. X-ray single-crystal diffraction analyses of **1** and **2** reveal azo-hydrazone tautomerism before and after metal-ion complexation, and UV–vis spectral comparison of **1** and **2** demonstrates strong hyperchromic effects after metal-ion complexation because of the formation of an additional electron-attracting phenolic group and stable fused five-membered and six-membered chelating rings. To the best of our knowledge, this is the first structural report about the heterocyclic dyes having quinoline-2,4-dione skeleton and the corresponding azo-hydrazone tautomerism between them.

Acknowledgments

We acknowledge the Major State Basic Research Development Program (Nos. 2011CB933300, 2007CB925101 and 2011CB808704), the NSFC (Nos. 20871065 and 21021062), and the Jiangsu Province project (No. BK2009226) for financial aid.

Appendix. Supplementary material

CCDC reference numbers 808425 and 808426 for **1** and **2** contain the supplementary crystallographic data for this paper. These data can be obtained free of charge at www.ccdc.cam.ac.uk/conts/retrieving.html [or from the Cambridge Crystallographic Data Centre, 12, Union Road, Cambridge CB2 1EZ, UK; Fax: (internat.) +44-1223/336-033; E-mail: deposit@ccdc.cam.ac.uk].

Supplementary data associated with this article can be found in the online version, at doi:10.1016/j.dyepig.2011.03.017.

References

[1] Venkataraman K. The chemistry of synthetic dyes, vol. I. New York: Academic Press; 1952. pp. 551–69. Chapter XIV.
[2] Zollinger H. Color chemistry: synthesis, properties and applications of organic dyes and pigments. 3rd revised ed. Weinheim, Germany: Wiley-VCH; 2003.
[3] Towns AD. Developments in azo disperse dyes derived from heterocyclic diazo components. Dyes and Pigments 1999;42(1):3–28.
[4] Geng J, Tao T, Fu SJ, You W, Huang W. Structural investigations on four heterocyclic Disperse Red azo dyes having the same benzothiazole/azo/benzene skeleton. Dyes and Pigments 2011;90:65–70.
[5] Pereira L, Coelho AV, Viegas CA, Santos MMC, Robalo MP, Martins LO. Enzymatic biotransformation of the azo dye Sudan Orange G with bacterial CotA-laccase. Journal of Biotechnology 2009;139(1):68–77.
[6] Wu SJ, Qian W, Xia ZJ, Zou YG, Wang SQ, Shen SY, et al. Investigation of third-order nonlinearity of an azo dye and its metal-substituted compounds. Chemical Physics Letters 2000;330(5–6):535–40.
[7] Zhang YQ, Martinez-Perdiguero J, Baumeister U, Walker C, Etxebarria J, Prehm M, et al. Laterally azo-bridged H-Shaped ferroelectric dimesogens for second-order nonlinear optics: ferroelectricity and second harmonic generation. Journal of the American Chemical Society 2009;131(51):18386–92.

[8] Abe T, Mano S, Yamada Y, Tomotake A. Thermal dye transfer printing with chelate compounds. Journal of Imaging Science and Technology 1999;43(4): 339–44.
[9] Nishihara H. Multi-mode molecular switching properties and functions of azo-conjugated metal complexes. Bulletin of the Chemical Society of Japan 2004; 77(3):407–28.
[10] Geng Y, Gu D, Gan F. Application of novel azo metal thin film in optical recording. Optical Materials 2004;27(2):193–7.
[11] Freeman HS, Posey JC. An approach to the design of lightfast disperse dyes-analogs of disperse yellow 42. Dyes and Pigments 1992;20(3):171–95.
[12] Wang S, Shen S, Xu H. Synthesis, spectroscopic and thermal properties of a series of azo metal chelate dyes. Dyes and Pigments 2000;44(3):195–8.
[13] Idelson M, Karady IR, Mark BH, Rickter DO, Hooper VH. Chromium complexes of o, o′-dihydroxyazo dyes: some chemistry of 1:1 complexes. Inorganic Chemistry 1967;6(3):450–8.
[14] Nejati K, Rezvani Z, Seyedahmadian M. The synthesis, characterization, thermal and optical properties of copper, nickel, and vanadyl complexes derived from azo dyes. Dyes and Pigments 2009;83(3):304–11.
[15] Kumar M, Babu JN, Bhalla V, Dhir A. Chromogenic sensing of Cu(II) by imino linked thiacalix[4]arene in mixed aqueous environment. Inorganic Chemistry Communications 2009;12:332–5.
[16] Lye J, Freeman HS, Mason ME, Singh P. X-ray crystal structure of CI Disperse Yellow 86. Dyes and Pigments 1999;42(1):107–11.
[17] Pavlovic G, Racane L, Cicak H, Tralic-Kulenovic V. The synthesis and structural study of two benzothiazolyl azo dyes: X-ray crystallographic and computational study of azo-hydrazone tautomerism. Dyes and Pigments 2009;83(3): 354–62.
[18] Seferoglu Z, Ertan N, Kickelbick G, Hokelek T. Single crystal X-ray structure analysis for two thiazolylazo indole dyes. Dyes and Pigments 2009;82(1): 20–5.
[19] Huang W, Qian HF. Structural characterization of C.I. Disperse Yellow 114. Dyes and Pigments 2008;77(2):446–50.
[20] Huang W. Structural and computational studies of azo dyes in the hydrazone form having the same pyridine-2,6-dione component (II): C.I. Disperse Yellow 119 and C.I. Disperse Yellow 211. Dyes and Pigments 2008;79(1):69–75.
[21] Qian HF, Huang W. An azo dye molecule having a pyridine-2,6-dione backbone. Acta Crystallographica, Section C: Crystal Structure Communications 2006;C62(2):o62–4.
[22] You W, Zhu HY, Huang W, Hu B, Fan Y, You XZ. The first observation of azo-hydrazone and cis-trans tautomerisms for Disperse Yellow dyes and their nickel(II) and copper(II) complexes. Dalton Transactions 2010;39(34): 7876–80.
[23] Tamasi G, Chiasserini L, Savini L, Sega A, Cini R. Structural study of ribonucleotide reductase inhibitor hydrazones. Synthesis and X-ray diffraction analysis of a copper(II)-benzoylpyridine-2-quinolinyl hydrazone complex. Journal of Inorganic Biochemistry 2005;99(6):1347–59.
[24] Siemens. SAINT v4 software reference manual. Madison, Wisconsin, USA: Siemens Analytical X-Ray Systems, Inc.; 2000.
[25] Sheldrick GM. SADABS, program for empirical absorption correction of area dectector data. Germany: Univ. of Gottingen; 2000.
[26] Siemens. SHELXTL, Version 6.10 reference manual. Madison, Wisconsin, USA: Siemens Analytical X-Ray Systems, Inc.; 2000.
[27] Park H, Kim ER, Kim DJ, Lee H. Synthesis of metal-azo dyes and their optical and thermal properties as recording materials for DVD-R. Bulletin of the Chemical Society of Japan 2002;75(9):2067–70.
[28] Chen W, Wu Y, Gu D, Gan F. Synthesis, optical and thermal characterization of novel thiazolyl heterocyclic azo dye. Materials Letters 2007;61(19–20): 4181–4.
[29] Gur M, Kocaokutgen H, Tasx M. Synthesis, spectral, and thermal characterizations of some azo-ester derivatives containing a 4-acryloyloxy group. Dyes and Pigments 2007;72(1):101–8.
[30] Chu W, Wai C. Effects of uv-decolouring of aromatic dyes with different chemical structures. Toxicological & Environmental Chemistry 1997;63(1): 247–55.
[31] Adachi M, Bredow T, Jug K. What is the origin of color on metal complex dyes? Theoretical analysis of a Ni-coordinate azo dye. Dyes and Pigments 2004; 63(3):225–30.
[32] Odabasoglu M, Arslan F, Olmez H, Buyukgungor O. Synthesis, crystal structures and spectral characterization of trans-bisaquabis(o-vanillinato)copper(II), cis-aquabis (o-vanillinato)copper(II) and aqua bis(o-vanillinato)-1,2-ethylenediimin copper(II). Dyes and Pigments 2007;75(3):507–15.
[33] Chen ZM, Wu YQ, Gu DH, Gan FX. Nickel(II) and copper(II) complexes containing 2-(2-(5-substitued isoxazol-3-yl)hydrazono)-5,5-dimethylcyclohexane-1,3-dione ligands: Synthesis, spectral and thermal characterizations. Dyes and Pigments 2008;76:624–31.
[34] Addison AW, Rao TN, Reedijk J, Vanrijn J, Verschoor GC. Synthesis, structure, and spectroscopic properties of copper(II) compounds containing nitrogen–sulphur donor ligands; the crystal and molecular structure of aqua[1,7-bis(N-methylbenzimidazol-2′-yl)-2,6-dithiaheptane]copper(II) perchlorate. Journal of the Chemical Society, Dalton Transactions 1984;7:1349–56.